Mol Neurobiol (2017) 54:6426–6435
DOI 10.1007/s12035-016-0185-8

Downregulation of Aquaporin-4 Protects Brain Against Hypoxia Ischemia via Anti-inflammatory Mechanism

Sujuan Liu[1,2] · **Juan Mao**[1] · **Tinghua Wang**[3] · **Xuemei Fu**[1]

Received: 25 April 2016 / Accepted: 30 September 2016 / Published online: 10 October 2016

Abstract Aquaporin-4 (AQP4), a water-channel protein, controls water fluxes into and out of the brain parenchyma. The role of AQP4 in brain edema formation and resolution remains controversial. This study therefore determined the roles of AQP4 in brain edema and explored the underlying molecular mechanism. We established hypoxia-ischemia (HI) neonatal rat model in vivo and HI cell model in vitro, which were administrated with lentiviral or shRNA vector, respectively. We found that the neurologic deficit and motor dysfunction could be induced by HI with more serious brain damage after longer HI time, and swollen cells with enlarged surrounding space were observed after HI induction. The quantity of water in the brain tissues was significantly increased in the HI rats when compared with the control group. However, the downregulation AQP4 by lentiviral or shRNA vector reversed the brain edema and neurologic deficit induced by HI. The underlying mechanism of beneficial effects of AQP4 downregulation may be due to interactive regulation of AQP4 and inflammatory cytokines including IL-1β, IL-6, IL-10, and TNFα. Our data demonstrate that the silence of AQP4 results in a significant decrease in the expression of IL-1β, IL-10, and TNFα, but had no direct effect on IL-6 expression. AQP4 could indirectly regulate the expression of IL-6 via IL-1β, IL-10, and TNFα. In summary, these findings provide a novel mechanism to explain the role of AQP4 in HI pathogenesis and are instrumental for the development of treatment for HI-induced brain edema.

Keywords Aquaporin-4 · Hypoxia-ischemia · Astrocyte · Brain edema · Inflammation

Introduction

Cerebral edema, an abnormal increase in brain water content, usually leads to an increase in intracranial pressure (ICP), brain ischemia, herniation, and death [1]. Regarding the brain edema resulting from an imbalance of water transportation in cells or blood vessels, maintenance of the balance of water transport between extracellular and intracellular is the key element. The discovery of aquaporins (AQPs) has provided a molecular basis for understanding water transport in several tissues, including the nervous system [2, 3].

Aquaporin-4 (AQP4), a member of AQPs family, is a water-channel protein expressed predominantly in astrocyte foot processes at the borders between the brain parenchyma and major fluid compartments, suggesting that AQP4 controls water fluxes into and out of the brain parenchyma [4–6]. However, the regulatory roles of AQP4 in the water balance of the central nervous system (CNS) are diverse under different physiology conditions.

Recent studies have indicated a key role of AQP4 in brain edema formation and resolution [7, 8]. But these studies have provided conflicting roles of AQP4 in brain edema. Downregulation of AQP4 has a beneficial role in brain edema produced by brain ischemia or meningitis [9]. AQP4 knockdown may protect against water influx in the formation of astrocyte swelling during hypoxia ischemia and may also delay water clearance in the resolution of astrocyte swelling

✉ Xuemei Fu
fxmzj2004@163.com

[1] Shenzhen Children's Hospital, Shenzhen, Guangdong 710038, China

[2] Department of Anatomy and Histology, School of Basic Medical Science, Tianjin Medical University, Tianjin 300070, China

[3] Institute of Neurological Disease, Translational Neuroscience Center, West China Hospital, Sichuan University, Chengdu 610041, China

during reoxygenation in vitro [10]. In the adult mouse stroke model, AQP4 deletion has a protective role from edema, suggesting that AQP4 may increase edema [11, 12]. However, in the juvenile rat HI models, the over-expression of AQP4 decreases brain edema [13]. Based on these findings, the exact roles of AQP4 in brain edema formation and resolution remain unclear and need to be solved urgently.

Recent studies have indicated an increased inflammatory response associated with brain swelling [14–18]. Lipopolysaccharide (LPS) treatment prior to hypoxia challenge causes cerebral edema, which was associated with an increase in TNFα, IL-1β, and IL-6 expression in cultured rat microglia via NF-κB and cAMP/PKA pathways [14]. The expression of several pro-inflammatory cytokines, including TNFα, IL-1β, IL-6, and NF-κB, is increased in HI rat model established by left common carotid artery ligation [15]. In addition, premature infants under hypoxic conditions may show increased expression of inflammatory factors such as TNFα and IL-6 [16]. Hypertonic saline can alleviate cerebral edema by inhibiting TNFα and IL-1β-induced Na-K-Cl cotransporter upregulation [17]. In neonates, cerebral hypoxia-ischemia (HI) is the primary cause of brain edema that leads to neurodevelopmental disabilities [19]. Therefore, we used neonatal rat HI model and cell model to investigate the functional interaction between AQP4 and inflammatory factors in HI-induced brain edema.

Methods

Hypoxia-Ischemia Animal Model

Animal Groups

This study was in accordance with the National Institute of Health guidelines for the treatment of animals and all experiments were approved by the guide for the Care and Use of Laboratory Animals of Tianjin Medical University, Tianjin, China. Sixty postnatal day-3 Sprague-Dawley (SD) rats (~8 g) were randomly divided into the following groups: sham groups, hypoxia ischemia groups for 4-h (HI 4 h, $n = 12$), 8-h (HI 8 h, $n = 12$), 16-h (HI 16 h, $n = 12$), and 24-h (HI 24 h, $n = 12$).

Animal Treatment

HI animal model was produced as described previously [20]. Briefly, after anesthesia by using inhalation diethylether, 3-day-old SD rat pups were fixed in a supine position and underwent the right carotid artery ligation with 5–0 silk through a longitudinal midline neck incision. The procedure lasted less than 5 min and the incision site was infiltrated with 2 % lidocaine. Following surgery, rats were returned to their mother for recovery and feeding for 30 min. Then, the pups were exposed for hypoxia (8 % O_2, 92 % N_2) by placing them in an air-tight chamber at a constant 37 °C. Sham operation was also put silk around common carotid artery, but not ligated. The rats in HI groups were further divided into four subgroups and sacrificed at 4, 8, 16, and 24 h later, respectively.

Hematoxylin and Eosin (HE) Staining

The biopsies of the cortex tissue, obtained at the scheduled time points, were submitted to routine hematoxylin-eosin analysis. A piece of the cortex tissue (0.1 cm^3) was cut, washed in phosphate-buffered saline (PBS), dehydrated with gradient alcohol, cleared with xylene, immersed in paraffin, and then embedded. Finally, 4-μm paraffin sections from this tissue were prepared for HE staining.

Assessment of Neurobehavioral Deficits

Neurologic examinations were performed 4, 8, 16, and 24 h after HI treatment by longa score scale. Longa score scale shows the grading of severity of brain function. The neurologic findings were scored on a five-point scale (Table 1).

Detection of Water Quantity in the Brain Tissue

For each group, the brains of six rat pups were harvested. The tissue was incised along sagittal suture. After the wet weight was measured, the tissue was then dried at 100 °C for 24 h, and its dry weight was measured. Water quantity of brain content (as a percentage) = (wet weight − dry weight)/wet weight × 100 %.

Immunofluorescence Analysis

The brain from HI24h group was obtained and placed in 20 % sucrose solution in 0.1 M phosphate buffer (PB). After the specimens had sunk to the bottom of the bottle, they were placed on a freezing microtome (Leica CM1900, Wetzlar, Hesse, Germany) and serial horizontal sections were cut at 12 μm thickness. For consistent representation of the data, five sections, the 10th, 20th, 30th, 40th, and 50th sections of

Table 1 Longa score scale

Score	Grading	Profile
0	No deficit	Normal
1	Mild	Failure to extend left forepaw fully
2	Moderate	Circling to the left
3	Severe	Falling to the left
4	Severe	No spontaneous walk and had a depressed level of consciousness

each animal, were stained with rabbit anti-GFAP antibody (1:200; Santa Cruz, Delaware, CA) at 4 °C for 24 h. After washing, sections were incubated with fluorescence-labeled secondary antibody IgG (anti-rabbit Cy3: red) for 4 h at 37 °C. The control sections were incubated in PBS to replace the primary antibody. After mounting, slides were observed by fluorescence microscopy.

Construction of RNA Interference Expression Vectors

Prepared siRNA Vectors

Three candidate target sequences of shRNA vectors were designed and synthesized by Ruibo Company GuangZhou, China. The sequence information was showed in Table 2. We examined AQP4, IL-1β, IL-6, IL-10, and TNFα gene expression to find the siRNA with the most significant inhibitory effect.

Primary Culture of Rat Cerebral Astrocytes

The cortex was gently separated from 1~3-day-old neonatal rat pups, and the meninges were gently peeled. Cortices were dissociated into a cell suspension using mechanical digestion. Then, cells were plated in 75 cm^2 tissue culture flasks with modified DMEM/F12 culture media at a concentration of 1.5×10^6 cells/ml. Incubating at 37 °C in a moist 5 % CO_2 atmosphere for 72 h before moving provided the cells sufficient time to adhere and begin multiplying. Flasks were shaken at 350 rpm for 6 h at 35 °C to separate the oligodendrocytes from the astrocytes, and then changed with fresh medium, and were shaken for another 18 h for harvested purified astrocytes.

siRNA Transfection

Astrocytes were transfected by three candidate target sequences of AQP4, IL-1β, IL-6, IL-10, and TNFα siRNA vectors to select the one with the maximum interference efficiency. Experiment was designed to include the following groups: normal group, tansfection reagent group, scrambled siRNA group, and target siRNA group. Transfection protocol was performed according to the manufacturer's instruction. Briefly, after 80 % confluent of cells, 4-μl siRNA vectors and 3-μl transfection reagent diluted with 100 μl transfection buffer were transfected into astrocytes. Cells were incubated for 12 h, exchanged fresh medium and subcultured at incubator. After 2, 4, and 7 days transfection, cell samples were collected for gene analysis.

Quantitative RT-PCR

Total RNA was extracted from cortex tissue using Trizol reagent (superfecTRI) according to the manufacturer's protocol and reversed transcription to cDNA with the RevertAid™ First Strand cDNA Synthesis kit (TaKaRa Biotechnology). For QRT-PCR, the primer sequences were shown as Table 3. PCR was performed in a DNA thermal cycler (ABI 7300) according to the following standard protocol: one cycle of 95 °C for 2 min; 40 cycles of 95 °C for 15 s, annealing for 20 s, and 60 °C for 40 s. Relative expressions were calculated with normalization to β-actin values by using the $2^{-\Delta\Delta Ct}$ method.

Preparation of Lentiviral Vector

To construct AQP4 recombinant lentiviral vector, the segment of highest interference efficiency was insert into pcDNAIII plasmid, then enveloped by HIV, by routing method. Briefly, segment sequence of highest interference efficiency was provided to GeneCopoeia, GuangZhou, China and constructed AQP4-lentiviral expression vector (AQP4-RNAi-LV). Thereafter, the rat AQP4 expression vector (5 μg) and viral packaging vectors (1 μl) were co-transfected into 293 T cells to produce lentiviral particles. The viral supernatant was harvested at 48 h post-transfection and filtered through a 0.45-μm cellulose acetate filter. Then, the 5 ml cell supernatant containing lentivirus was centrifuged (3500*g*, 25 min). And the precipitate was re-dissolved in 500 μl PBS. Finally, the recombinant AQP4-RNAi-LV was stored at −80 °C till use. The control plasmid was also packaged, designated as no-targeting-LV.

Table 2 Sequence information of siRNA vectors

Name	F1 target sequences	F2 target sequences	F3 target sequences
AQP4	CCAAGTCCGTCTTCTACAT	CAGGTGCACTTTACGAGTA	CAGCATGAATCCAGCTCGA
IL-1β	GGAAGGCAGTGTCACTCAT	GCACAGACCTGTCTTCCTA	CTGCAGGCTTCGAGATGAA
IL-6	GAAAGCACTTGAAGAATTT	GAAACTTCCAGAAATACAA	CAGGAAATTTGCCTATTGA
IL-10	CATAGAAGCCTACGTGACA	ACAACATACTGCTGACAGA	CCATGAATGAGTTTGACAT
TNFα	CCCACAACGAGGACTACA	CGTGAAGAATGTGCGAGAC	GCCCGTAGCCCACGTCGTA

Table 3 Detailed information on the selection of primers for QRT-PCR experiments

Name	Primer sequence (sense)	Primer sequence (antisense)
β-actin	GAAGATCAAGATCATTGCTCCT	TACTCCTGCTTGCTGATCCA
AQP4	GACATTTGTTTGCAATCAAT	AACCCAATATATCCAGTGGTT
IL-1β	GAGCTGAAAGCTCTCCACCT	TTCCATCTTCTTCTTTGGGT
IL-6	AGAAGACCAGAGCAGATTTT	GAGAAAAGAGTTGTGCAATG
IL-10	CAGAAATCAAGGAGCATTTG	CTGCTCCACTGCCTTGCTTT
TNFα	GCCCACGTCGTAGCAA	GTCTTTGAGATCCATGCCAT

Injection of AQP4-RNAi-LV in Cortex In Vivo

AQP4-RNAi-LV Transduction of Brain Tissue In Vivo

HI neonatal rats were randomly assigned to no-targeting-LV and AQP4-RNAi-LV group (n = 8). The animal was deeply anesthetized and fixed in a stereotaxic apparatus. The dorsal surface of the skull was then exposed and cleaned. And lentivirus (4 μl) was injected in cerebral cortex motor area of hemisphere. The skin was sutured after surgery. Animals were given the optimum temperature and maintained in cage comfortable.

Verification of the Interference Efficiency of AQP4-RNAi-LV by Western Blotting Analysis

Brain tissue injected by AQP4-RNAi-LV was removed to extract protein and detect AQP4 expression. Protein samples were boiled for 10 min and fractionated on 15 % SDS-PAGE gels. After electrophoresis for 120 min at 75 V, the proteins were transferred to PVDF membranes (Millipore). The membranes were then blocked in 5 % nonfat milk in PBS for 120 min at room temperature and incubated with primary antibody of AQP4 (Santa Cruz Biotechnology), diluted 1:1000 in TBS overnight at 4 °C. After washed in three changes of PBS, the membranes were incubated for 2 h with secondary antibody (goat anti-rabbit IgG) diluted 1:5000. Finally, the immune complexes were revealed using Alpha Innotech (Bio-Rad) with ECL.

Behavior Analyses and Astrocytes Morphology Change after Lentivirus Injection

The blinded longa scale score test for neural impairment was performed after AQP4-RNAi-LV injection, as described in the dedicated paragraph. To examine the changes of astrocyte morphology following AQP4-RNAi-LV injection, the horizontal sections of brain tissue via injection point were performed immunofluorescence staining. A panel of primary antibodies included rabbit anti-GFAP (1:200) and mouse anti-AQP4 (1:100). Primary antibodies were detected using Cy3 (red) and dylight 488 (green)-conjugated secondary antibodies.

Statistical Analysis

All data were expressed as means ± S.E.M. Number of animals used is indicated by n. The significance of the difference between the groups was calculated by one-way analysis of variance followed by Fisher's least significant difference post hoc test. Probability values (P) of less than 0.05 were considered to significant differences.

Results

Detrimental Outcomes After Hypoxia Ischemia

Morphology of the brain tissues following HI was examined by HE straining under light microscopy. The space surrounding capillaries of cells widened slightly and no swelling or necrosis cells were observed in sham group. They looked morphologically normal with clear cell borders and nucleolus. In contrast, signs of edema were observed in the brain tissue of the HI groups (4 h, 8 h, 16 h, 24 h). Despite that the arrangement of nerve cells remained almost normal in HI group, the cells were swollen, decreased in number, lost polarity with abnormal circular shape, and the defects were more severe with longer time after hypoxic ischemic treatment. We also found increased space around cells, and the vacant area probably resulted from cell death (Fig. 1a). Consistent with the morphological data, the quantity of water in the brain tissues was significantly increased in the HI groups when compared with control group ($P < 0.05$) (Fig. 1b). To determine neural dysfunction induced by hypoxia ischemia, longa score scale was used to assess the neural function. Compared with the control group, the longa score was significantly increased in HI groups, indicating neurologic defect and motor dysfunction in HI rats with increased severity after longer time of HI (Fig. 1c).In addition, compared with sham group, the expression of AQP4 protein was significantly decreased after HI treatment ($P < 0.05$, $P < 0.01$; Fig. 1d).

HI Induces Astrocyte Swelling

To determine the effect of HI on the morphology of astrocytes, GFAP, a specific maker of astrocyte, was used to identify

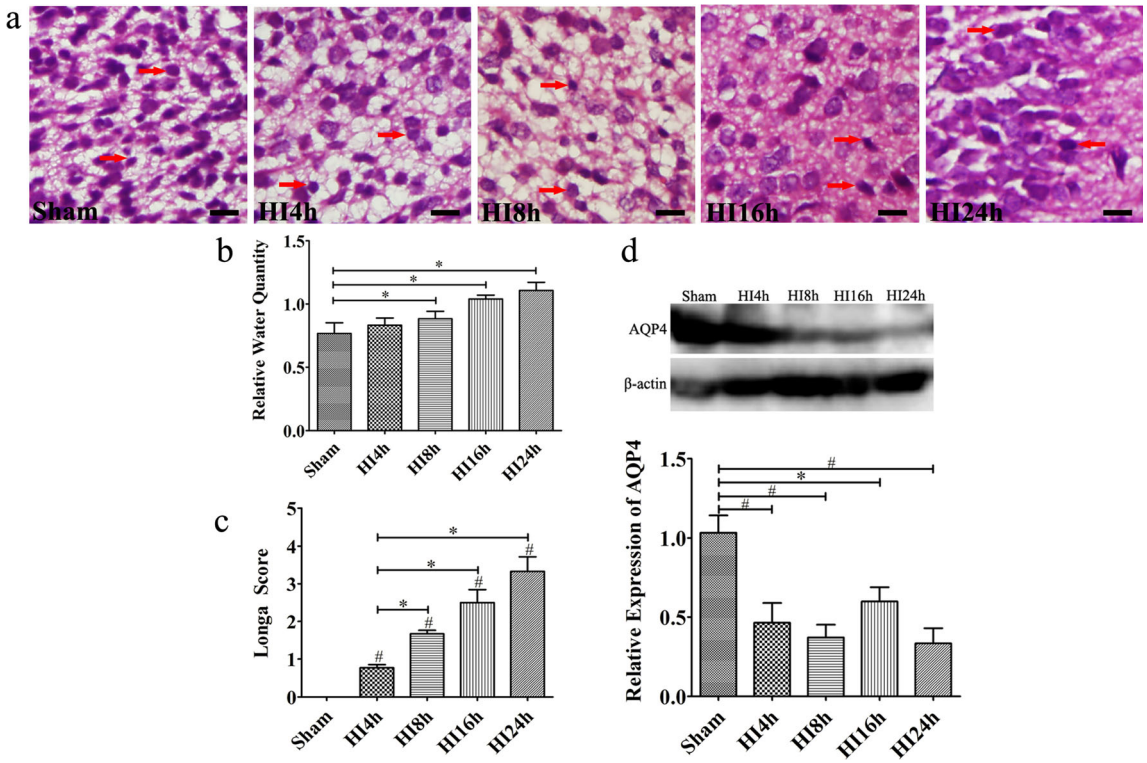

Fig. 1 Pathologies induced by HI. **a** HE staining analysis indicated that swollen cells, abnormally circular and enlarged space around cells, were observed following HI, and these defects were more severe with longer time of hypoxic ischemia (400×, 4 h, 8 h, 16 h, 24 h). At least five fields were analyzed in each case (n = 12). **b** Water quantity in the brain is increased significantly after HI when compared to the sham group. **c** The longa score scale was increased beginning 4 h after HI and sustained until 24 h. The extent of brain function damage was increased with the time of HI. **d** The expression of AQP4 was significantly decreased after HI compared with sham group. The *arrows* indicate the edema cells. *Bar* = 20 μm, shown in **a**. $^{*}P < 0.05$ and $^{\#}P < 0.01$

astrocytes. Compared with GFAP positive cells in sham group, the soma of GFAP positive cells subjected to HI for 24 h was greatly increased ($P < 0.01$), implying that astrocyte swelling was induced by HI (Fig. 2).

Selection of the Most Effective siRNA and the Optimal Time Point of Transfection

To select the most effective siRNA, three AQP4-siRNA sequences (F1, F2, F3) were transfected into astrocytes. Data indicate that the reduction of the expression of AQP4 by F1, F2, and F3 was 0.411, 0.767, and 1.035, respectively, indicating that F1 was the most effective AQP4-siRNA sequence to silence AQP4 expression (Fig. 3a). F1 was transfected into astrocytes to determine the silencing efficiency at different time points (2, 4, and 7 days) after transfection. The expression of AQP4 gene was significantly decreased 2 days after transfection into cells, while the effect of gene silencing was eliminated 4 and 7 days after transfection (Fig. 3b). We also identified the most effective siRNA sequence to silence the expression of IL-1β, IL-6, IL-10, and TNFα, respectively (data not shown).

Cell Swelling Was Reversed by AQP4 Silencing in Vitro

Astrocyte morphologic images were collected and observed by a phase contrast microscopy after 24 h HI and AQP4 siRNA administration. The size soma of astrocyte was significantly increased 24 h after HI ($P < 0.01$ vs. normal), but was significantly decreased following AQP4 siRNA administration ($P < 0.01$ vs. HI24h), suggesting that HI-induced cell swelling was reversed by AQP4 silencing (Fig. 3c, d).

Silencing AQP4 in Brain Tissue with Lentivirus Transduction

After AQP4-RNAi-LV was injected into rats' cortex, we confirmed the silencing effect on the expression of AQP4 by Western blotting and immunofluorescent staining. The expression of AQP4 was significantly decreased following AQP4-RNAi-LV injection ($P < 0.01$ vs. no-targeting-LV group), indicating that the expression of AQP4 protein was successfully silenced by lentiviral vector (Fig. 4a, b). As expected, the expression of AQP4 (green) was decreased and the cell soma size was smaller in the HI brain of AQP4-RNAi-LV group, suggesting that AQP4-RNAi-LV has successfully

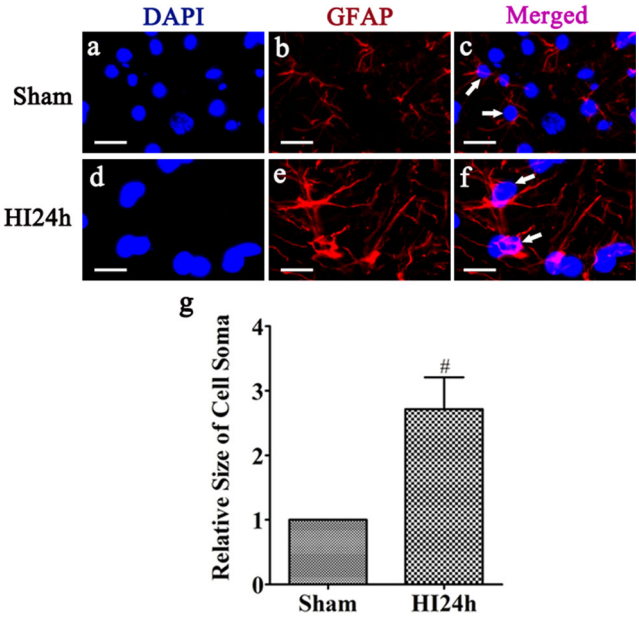

Fig. 2 Astroctyes swelling is induced by HI. Compared with the sham group (**a**–**c**), the size soma of astrocyte was significantly increased in HI24h group (**d**–**f**). DAPI staining is presented in **a** and **d**. GFAP staining is presented in **b** and **e**. Merged image is presented in **c** and **f**. Quantitative analysis of soma is shown in **g** ($n = 5$, $^{\#}P < 0.01$). The *arrows* indicate the edema positive GFAP cells. *Bar* = 50 μm

reduced the AQP4 expression and astrocyte swelling induced by HI (Fig. 4c, d). GFAP-positive cells (red) were simultaneously labeled by AQP4 antibody (green), indicating AQP4 expression in astrocytes (Fig. 4c, d).

Effect of Downregulation AQP4 on HI-Induced Pathologies In Vivo

HE staining was performed to assess the cell morphology changes of the brain tissue after HI following AQP4 interference; compared with the control group, AQP4 interference partially reversed the pathologic phenotypes induced by HI, including cell swelling, cellular necrosis, and illegible cellular borders (Fig. 4e). And longa score scale result showed that the downregulation of AQP4 could attenuate neural dysfunction induced by HI ($P < 0.05$ vs. no-targeting-LV group; Fig. 4f).

Interaction Between AQP4 and Inflammatory Factors

To further understand the roles of AQP4, qRT-PCR was performed to examine the AQP4, IL-1β, IL-6, IL-10, and TNFα expression following downregulation on one of them. Compared with control group, AQP4 interference resulted in a significant decrease of IL-1β, IL-10, and TNFα, but had no effect on IL-6 expression ($P < 0.01$; Fig. 5a). AQP4 and IL-6 were significantly increased following the silencing of IL-1β, IL-10, and TNFα when compared with control one ($P < 0.01$; Fig. 5b–e). While AQP4 was significantly increased after IL-6 interference, no significant difference was observed in IL-1β, IL-10, and TNFα expression after IL-6 silencing when compared with control group (Fig. 5c). Therefore, AQP4 could directly increase the expression of IL-1β, IL-10, and TNFα expression and indirectly decreased IL-6 expression. Moreover, IL-1β, IL-6, IL-10, and TNFα negatively regulated the expression of AQP4 (Fig. 5f).

Discussion

Brain edema is caused by abnormal water homeostasis following hypoxia ischemia [1, 21]. During the early events of HI, there are at least three causes for brain edema formation: (1) the permeability of sodium and potassium of the cell membrane is increased [22]; (2) the activation of transport pumps (Na/K ATPase pump) fails [23]; and (3) the osmotic pressure of cells is enhanced [23, 24]. Passive water transport into the

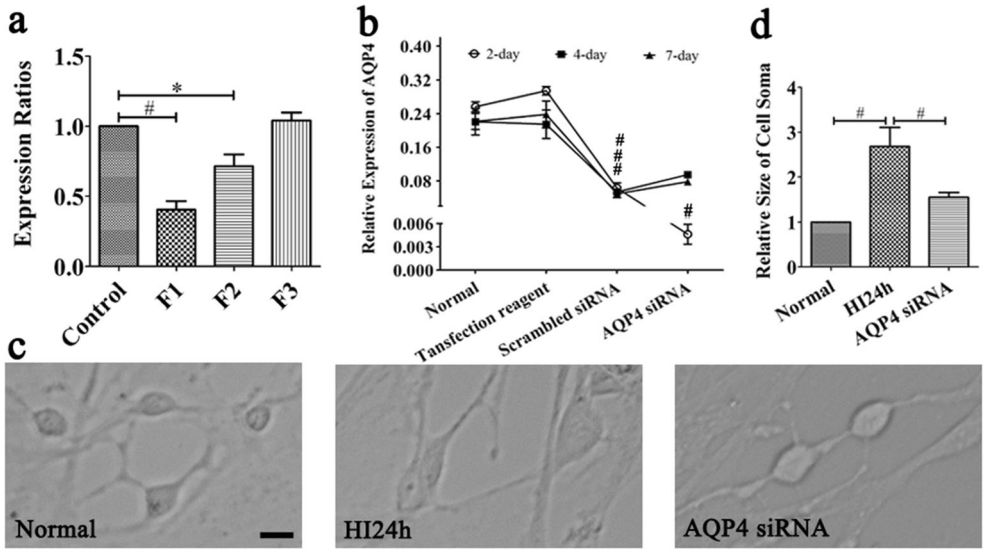

Fig. 3 Cellular swelling was reversed by AQP4 silencing in vitro. **a** Comparative analysis showed F1 was more effective in silencing AQP4 expression than F2 and F3. **b** AQP4 gene expression was significantly decreased 2 days after transfection of F1. **c**, **d** Morphologic analysis showed that the cellular swelling induced by HI was attenuated by AQP4 siRNA interference. *Bar* = 20 μm, shown in **c**. $^{*}P < 0.05$ and $^{\#}P < 0.01$

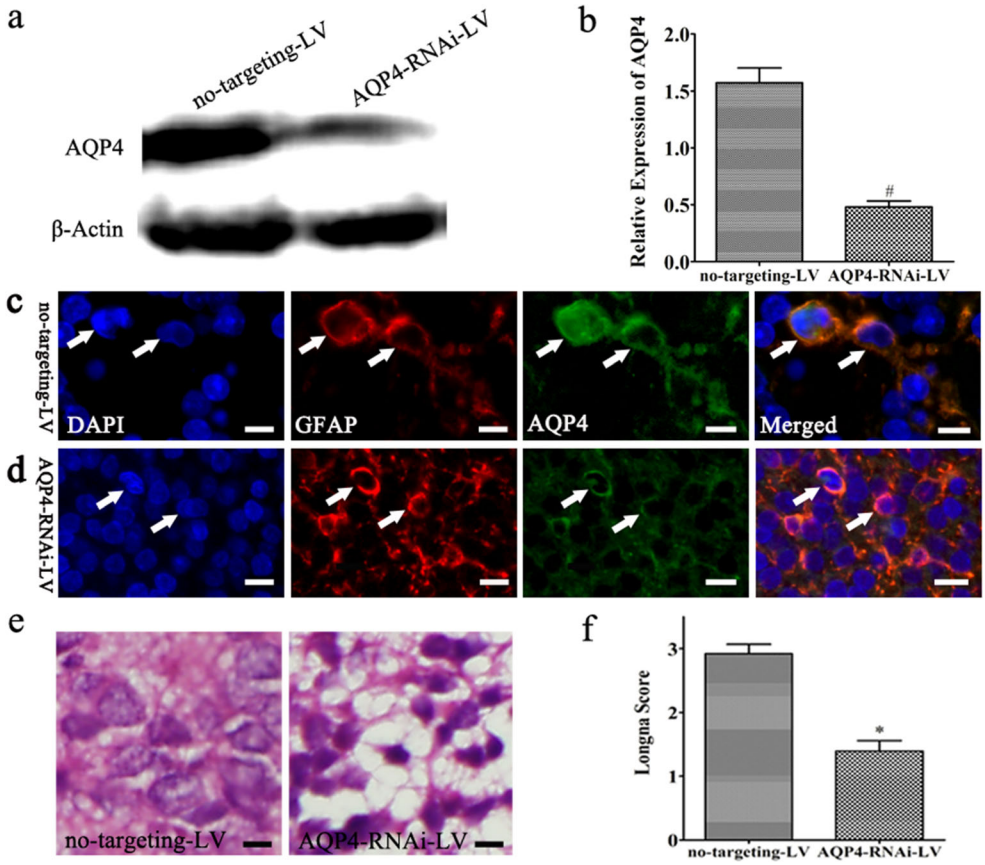

Fig. 4 Effects of AQP4 silencing on cell morphology and neural function in vivo. **a**, **b** Compared with the control (no-targeting-LV) group, the AQP4 protein levels were prominently decreased in AQP4-RNAi-LV group. Western blot bands were shown in **a**, and quantitative analysis was shown in **b** ($n = 5$, $^{\#}P < 0.01$). **c**, **d** GFAP-positive (*red*) cells were also positive for AQP4 (*green*), confirming that AQP4 was expressed in astrocytes. In addition, when compared with no-targeting-LV group, the green fluorescence and the size soma of astrocytes were remarkably decreased following AQP4 silencing. The *arrows* indicate the GFAP-positive astrocytes (*red*) and AQP4-positive cells (*green*). *Bar* 20 μm, shown in **c**–**e**. **e** HE straining analysis indicated brain edema induced by HI was relieved in AQP4 interference group. At least five fields were analyzed in each case. **f** Longa score scale data showed downregulation of AQP4 could attenuate neural dysfunction induced by HI. $^{*}P < 0.05$ and $^{\#}P < 0.01$

cell caused by the increased osmotic gradient results in brain edema. AQP4 is highly expressed in astrocytes throughout CNS, especially at the blood-brain and brain-cerebrospinal fluid barriers [6, 25], and plays multiple roles in water transport [11, 26]. Therefore, as a self-protective mechanism, a decrease in AQP4 expression reduces further water flowing into astrocytes and thus relieves cellular edema.

In this study, by establishing a brain edema HI rat model, which was developed by Rice and colleagues in 1981 [27], we examined in greater detail the HI-induced functional (neurologic deficit and motor dysfunction) and morphological (cell swollen, cell necrosis, and water quantity increased) changes at different time points (2, 4, and 7 days) after HI. Our results indicate that the combination of unilateral carotid artery ligation and hypoxia could be used to establish a HI model. A consistent AQP4 protein expression pattern was detected as in our previous study [10]. The protein expression of AQP4 was significantly decreased following HI in a time-dependent manner, suggesting a self-protective mechanism from cellular edema. Given that AQP4 is richly expression in astrocytes, we cultured the primary astrocytes originated from cerebral cortex of rat, and study AQP4 function and regulation. In addition, cell in vitro makes it a good candidate and excludes many complex pathological elements which exist in vivo. Therefore, we selected the highest inhibition rate of siRNA fragment and further examined the best time point of interference. Our results showed F1 had the highest inhibition efficiency and then was used to construct lentivirus vector of AQP4 for following research; considering the best inhibition efficiency for transfection at 2 days but not at 4 and 7 days, we remained hypoxia ischemia administration for 24 h.

To explore the exact effect of HI on astrocytes, immunofluorescence stain of GFAP was performed. Despite the arrangement of cells remained neat to some extent, the astrocytes were swollen, irregular shapes and fragmented nuclei. Quantitative analysis showed astrocytes soma was

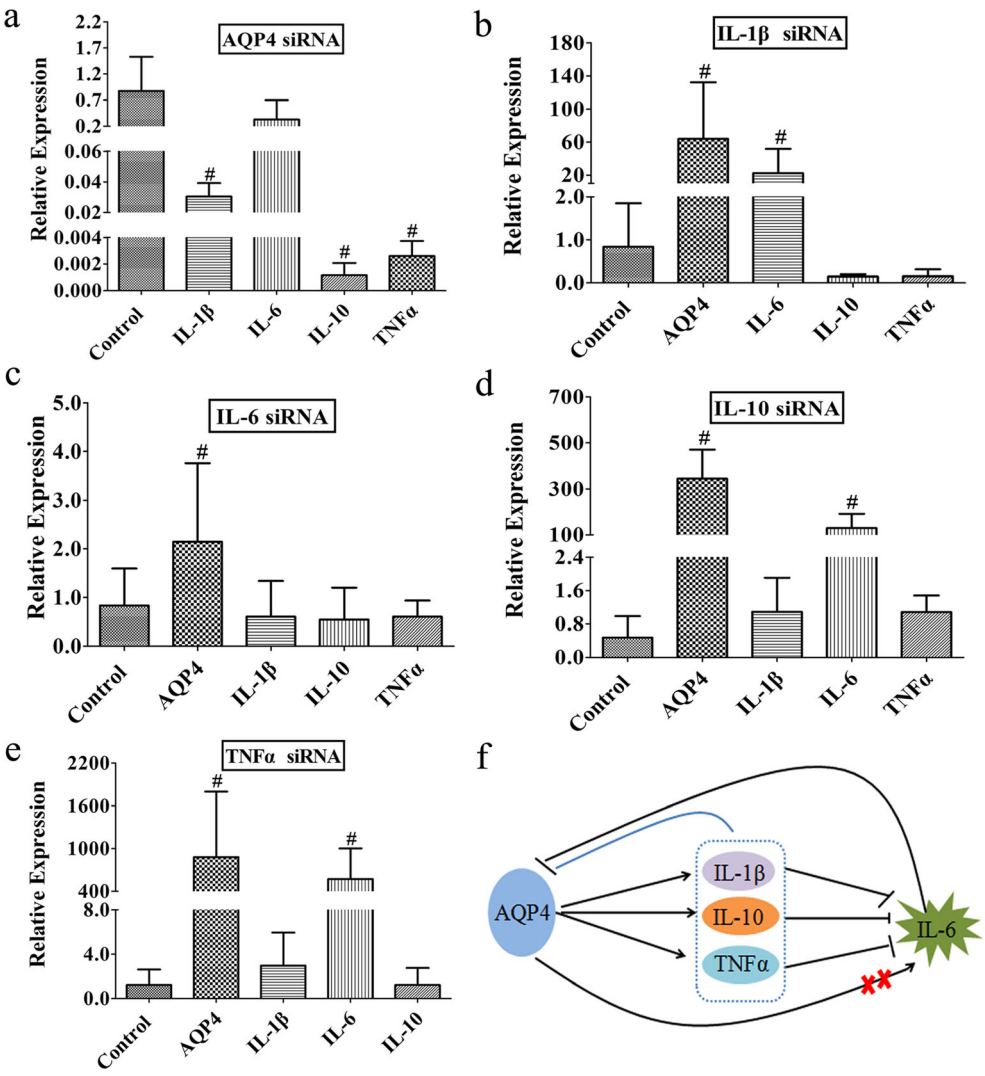

Fig. 5 Interaction between AQP4 and inflammatory factors including IL-1β, IL-6, IL-10, and TNFα. **a** Compared with the control group, AQP4 silencing results in a significant decrease in the expression of IL-1β, IL-10, and TNFα, but had no effect on IL-6. **b**, **d**, **e** AQP4 and IL-6 were significantly increased following IL-1β, IL-10, and TNFα interference when compared with control one. **c** The expression of AQP4 was significantly increased after IL-6 interference, which had no significant impact on IL-1β, IL-10, and TNFα expression. **f** The functional loop AQP4/IL-1β, IL-10, TNFα/IL-6 signaling pathways. $^{\#}P < 0.01$

significantly increased after 24 h of HI compared with control, consistent with the HE staining.

In further support of this notion, downregulation of AQP4 protein reverses the HI-induced brain edema, improving the neural function after HI. This conclusion also agrees with the observation that AQP4 promotes brain edema and AQP4 deletion reduces brain damage and brain swelling [14, 28]. Recent studies showed AQP4 expression was increased in response to HI and AQP4 enhanced water influx into astrocytes under HI pathological state [29, 30].

The fetal inflammatory response plays a pivotal role in the pathogenesis of preterm birth and neonate brain injury. A neuro-inflammatory response to infection in CNS and/or systemic inflammation is a likely cause of damage to the developing brain. The concurrent activation of anti-inflammatory mechanisms can provide negative feedback loops and generate neuroprotective and even repair mechanisms in the developing brain [31–34]. In this study, we unveil the underlying molecular mechanism of beneficial effects of the downregulation of AQP4, closely associated with anti-inflammatory response. In this context, our data show the expression of the inflammatory factors is significantly decreased after AQP4 interference, indicating AQP4 upregulates the expression of IL-1β, IL-10, and TNFα. Previously studies found that the expression of IL-1β and TNFα is increased significantly following HI encephalopathy of infants when compared to control [35]. Therefore, downregulation of IL-1β and TNFα expression could attenuate the development of brain edema. In addition, our data showed IL-6 was significantly increased following IL-1β, IL-10, and TNFα silencing, suggesting IL-6 is mediating downstream inflammatory response after HI. Consistent with this finding, our published data indicate that the downregulation of IL-1β protects the brain from edema induced by HI and is associated with increasing IL-6 expression [36]. In addition, we show that all those inflammatory factors negatively regulate AQP4. Therefore, AQP4 silencing could decrease IL-1β, IL-10, and TNFα expression, leading to increased IL-6

expression, which further suppress the expression of AQP4. We reason that the functional interaction between AQP4/IL-1β, IL-10, and TNFα/IL-6 signaling pathways plays important roles in water accumulation, transfer, and clearance in brain edema.

In conclusion, our findings demonstrated that AQP4 enhances water flux into astrocytes during brain edema induced by HI. In addition, the downregulation of AQP4 reverses the neural defects induced by HI through the functional loop involving AQP4/IL-1β, IL-10, and TNFα/IL-6 signaling pathways. These findings support the notion that silence of AQP4 expression may represent an attractive strategy in the therapy of brain edema followed HI in neonates.

Acknowledgments This study is supported by a grant from the National High-tech R&D Program (863 Program No. 2015AA020310), the National Natural Science Foundation of China (Nos. 81501071, 815300045, 81373166), Shenzhen Development and Reform Commission and Shenzhen Municipal Science and Technology Innovation Council (20140405201035).

Compliance with Ethical Standards

Conflict of Interest The authors declare that they have no conflict of interest.

References

1. Nico B, Ribatti D (2011) Role of aquaporins in cell migration and edema formation in human brain tumors. Exp Cell Res 317(17): 2391–2396. doi:10.1016/j.yexcr.2011.07.006
2. Sales AD, Lobo CH, Carvalho AA, Moura AA, Rodrigues AP (2013) Structure, function, and localization of aquaporins: their possible implications on gamete cryopreservation. Genet Mol Res 12(4):6718–6732. doi:10.4238/2013.December.13.5
3. Azuma M, Nagae T, Maruyama M, Kataoka N, Miyake S (2012) Two water-specific aquaporins at the apical and basal plasma membranes of insect epithelia: molecular basis for water recycling through the cryptonephric rectal complex of lepidopteran larvae. J Insect Physiol 58(4):523–533. doi:10.1016/j.jinsphys.2012.01.007
4. He Z, Wang X, Wu Y, Jia J, Hu Y, Yang X, Li J, Fan M et al (2014) Treadmill pre-training ameliorates brain edema in ischemic stroke via down-regulation of aquaporin-4: an MRI study in rats. PLoS One 9(1):e84602. doi:10.1371/journal.pone.0084602
5. Goodyear MJ, Crewther SG, Junghans BM (2009) A role for aquaporin-4 in fluid regulation in the inner retina. Vis Neurosci 26(2):159–165. doi:10.1017/s0952523809090038
6. Nagelhus EA, Ottersen OP (2013) Physiological roles of aquaporin-4 in brain. Physiol Rev 93(4):1543–1562. doi:10.1152/physrev.00011.2013
7. Papadopoulos MC, Verkman AS (2007) Aquaporin-4 and brain edema. Pediatr Nephrol 22(6):778–784. doi:10.1007/s00467-006-0411-0
8. Xu M, Su W, Xu QP (2010) Aquaporin-4 and traumatic brain edema. Chin J Traumatol 13(2):103–110
9. Wang BF, Cui ZW, Zhong ZH, Sun YH, Sun QF, Yang GY, Bian LG (2015) Curcumin attenuates brain edema in mice with intracerebral hemorrhage through inhibition of AQP4 and AQP9 expression. Acta Pharmacol Sin 36(8):939–948. doi:10.1038/aps.2015.47
10. Fu X, Li Q, Feng Z, Mu D (2007) The roles of aquaporin-4 in brain edema following neonatal hypoxia ischemia and reoxygenation in a cultured rat astrocyte model. Glia 55(9):935–941. doi:10.1002/glia.20515
11. Manley GT, Fujimura M, Ma T, Noshita N, Filiz F, Bollen AW, Chan P, Verkman AS (2000) Aquaporin-4 deletion in mice reduces brain edema after acute water intoxication and ischemic stroke. Nat Med 6(2):159–163. doi:10.1038/72256
12. Dmytrenko L, Cicanic M, Anderova M, Vorisek I, Ottersen OP, Sykova E, Vargova L (2013) The impact of alpha-syntrophin deletion on the changes in tissue structure and extracellular diffusion associated with cell swelling under physiological and pathological conditions. PLoS One 8(7):e68044. doi:10.1371/journal.pone.0068044
13. Meng S, Qiao M, Lin L, Del Bigio MR, Tomanek B, Tuor UI (2004) Correspondence of AQP4 expression and hypoxic-ischaemic brain oedema monitored by magnetic resonance imaging in the immature and juvenile rat. Eur J Neurosci 19(8):2261–2269. doi:10.1111/j.0953-816X.2004.03315.x
14. Song TT, Bi YH, Gao YQ, Huang R, Hao K, Xu G, Tang JW, Ma ZQ et al (2016) Systemic pro-inflammatory response facilitates the development of cerebral edema during short hypoxia. J Neuroinflammation 13(1):63. doi:10.1186/s12974–016–0528-4
15. Li D, Song T, Yang L, Wang X, Yang C, Jiang Y (2016) Neuroprotective actions of pterostilbene on hypoxic-ischemic brain damage in neonatal rats throughupregulation of heme oxygenase-1. Int J Dev Neurosci:22–31. doi:10.1016/j.ijdevneu.2016.08.005
16. Ambalavanan N, Carlo WA, McDonald SA, Das A, Schendel DE, Thorsen P, Hougaard DM, Skogstrand K, Higgins RD (2012) Cytokines and posthemorrhagic ventricular dilation in premature infants. Am J Perinatol29(9):731–40
17. Huang LQ, Zhu GF, Deng YY, Jiang WQ, Fang M, Chen CB, Cao W, Wen MY et al (2014) Hypertonic saline alleviates cerebral edema by inhibiting microglia-derived TNF-α and IL-1β-induced Na-K-Cl Cotransporter up-regulation. J Neuroinflammation 11:102. doi:10.1186/1742–2094–11-102
18. Lee JH, Espinera AR, Chen D, Choi KE, Caslin AY, Won S, Pecoraro V, Xu GY et al (2016) Neonatal inflammatory pain and systemic inflammatory responses as possible environmental factors in the development of autism spectrum disorder of juvenile rats. J Neuroinflammation 13(1):109. doi:10.1186/s12974-016-0575-x
19. Sameshima H, Ikenoue T (2013) Hypoxic-ischemic neonatal encephalopathy: animal experiments for neuroprotective therapies. Stroke Res Treat 2013:659374. doi:10.1155/2013/659374
20. Barks JD, Post M, Tuor UI (1991) Dexamethasone prevents hypoxic-ischemic brain damage in the neonatal rat. Pediatr Res 29(6):558–563. doi:10.1203/00006450-199106010-00008
21. Fang CZ, Yang YJ, Wang QH, Yao Y, Zhang XY, He XH (2013) Intraventricular injection of human dental pulp stem cells improves hypoxic-ischemic brain damage in neonatal rats. PLoS One 8(6): e66748. doi:10.1371/journal.pone.0066748
22. Garrett MC, Komotar RJ, Starke RM, Merkow MB, Otten ML, Sciacca RR, Connolly ES (2009) The efficacy of direct extracranial-intracranial bypass in the treatment of symptomatic hemodynamic failure secondary to athero-occlusive disease: a systematic review. Clin Neurol Neurosurg 111(4):319–326. doi:10.1016/j.clineuro.2008.12.012
23. Chipperfield AR, Harper AA (2000) Chloride in smooth muscle. Prog Biophys Mol Biol 74(3–5):175–221
24. Davalos A, Shuaib A, Wahlgren NG (2000) Neurotransmitters and pathophysiology of stroke: evidence for the release of glutamate and other transmitters/mediators in animals and humans. J Stroke Cerebrovasc Dis 9(6 Pt 2):2–8. doi:10.1053/jscd.2000.18908

25. Iacovetta C, Rudloff E, Kirby R (2012) The role of aquaporin 4 in the brain. Vet Clin Pathol 41(1):32–44. doi:10.1111/j.1939-165X.2011.00390.x
26. Manley GT, Binder DK, Papadopoulos MC, Verkman AS (2004) New insights into water transport and edema in the central nervous system from phenotype analysis of aquaporin-4 null mice. Neuroscience 129(4):983–991. doi:10.1016/j.neuroscience.2004.06.088
27. Rice JE 3rd, Vannucci RC, Brierley JB (1981) The influence of immaturity on hypoxic-ischemic brain damage in the rat. Ann Neurol 9(2):131–141. doi:10.1002/ana.410090206
28. Chang KH, Yeh CM, Yeh CY, Huang CC, Hsu KS (2013) Neonatal dexamethasone treatment exacerbates hypoxic-ischemic brain injury. Mol Brain 6:18. doi:10.1186/1756-6606-6-18
29. Sun MC, Honey CR, Berk C, Wong NL, Tsui JK (2003) Regulation of aquaporin-4 in a traumatic brain injury model in rats. J Neurosurg 98(3):565–569. doi:10.3171/jns.2003.98.3.0565
30. Papadopoulos MC, Verkman AS (2005) Aquaporin-4 gene disruption in mice reduces brain swelling and mortality in pneumococcal meningitis. J Biol Chem 280(14):13906–13912. doi:10.1074/jbc.M413627200
31. Malaeb S, Dammann O (2009) Fetal inflammatory response and brain injury in the preterm newborn. J Child Neurol 24(9):1119–1126. doi:10.1177/0883073809338066
32. Lee JH, Wei ZZ, Cao W, Won S, Gu X, Winter M, Dix TA, Wei L, Yu SP (2016) Regulation of therapeutic hypothermia on inflammatory cytokines, microglia polarization, migration and functional recovery after ischemic stroke in mice. Neurobiol Dis96:248–260. doi: 10.1016/j.nbd.2016.09.013
33. Bastek JA, Gómez LM, Elovitz MA (2011) The role of inflammation and infection in preterm birth. Clin Perinatol 38(3):385–406. doi:10.1016/j.clp.2011.06.003
34. Chevin M, Guiraut C, Maurice-Gelinas C, Deslauriers J, Grignon S, Sébire G (2016) Neuroprotective effects of hypothermia in inflammatory-sensitized hypoxic-ischemic encephalopathy. Int J Dev Neurosci:1–8. doi:10.1016/j.ijdevneu.2016.09.002
35. Liu F, McCullough LD (2013) Inflammatory responses in hypoxic ischemic encephalopathy. Acta Pharmacol Sin 34(9):1121–1130. doi:10.1038/aps.2013.89
36. Liu S, Zhu S, Zou Y, Wang T, Fu X (2015) Knockdown of IL-1beta improves hypoxia-ischemia brain associated with IL-6 up-regulation in cell and animal models. Mol Neurobiol 51(2):743–752. doi:10.1007/s12035-014-8764-z